論文 / 著書情報
Article / Book Information

Title	Influence of initial fines content on fabric of soils subjected to internal erosion
Authors	Mao Ouyang, Akihiro Takahashi
Citation	Canadian Geotechnical Journal, Vol. 53, No. 2, pp. 299-313
Pub. date	2016, 2
DOI	http://dx.doi.org/10.1139/cgj-2014-0344
Note	This file is author (final) version.

Influence of initial fines content on fabric of soils subjected to internal erosion

Mao Ouyang, Akihiro Takahashi

M. Ouyang. Department of Civil Engineering, Tokyo Institute of Technology, 2-12-1-M1-3 Oh-okayama, Meguro, Tokyo 152-8552, Japan. (e-mail: ouyang.m.aa@m.titech.ac.jp)

A. Takahashi. Department of Civil Engineering, Tokyo Institute of Technology, 2-12-1-M1-3 Oh-okayama, Meguro, Tokyo 152-8552, Japan. (e-mail: takihiro@cv.titech.ac.jp)

Corresponding author: Akihiro Takahashi (e-mail: takihiro@cv.titech.ac.jp)

Canadian Geotechnical Journal, 53(2), 299-313, 2016

Original URL:

http://dx.doi.org/10.1139/cgj-2014-0344

Abstract: Seepage-induced internal erosion often happens in earth structures. This paper presents experimental investigations on the influence of initial fines content on fabric of soils subjected to internal erosion. The tested materials were the binary mixtures of silica No. 3 and silica No. 8, which correspond to the coarse and fine fractions, respectively. One group of specimens was prepared with initial fines contents of 0, 15%, 25%, and 35% by weight. The undrained monotonic compression tests were performed on this group to examine the influence of fines content on the undrained behavior. The other group was prepared with initial fines contents of 15%, 25%, and 35% by weight, on which the seepage tests and subsequent undrained compression tests were carried out to demonstrate the mechanical influence of the internal erosion. The undrained behavior of the first group of specimens reveals that the presence of fines would decrease the peak and residual strengths. A comparison between the undrained behavior of soils with erosion and that of soils without erosion shows that the soils become less contractive after the internal erosion. When the axial strain is less than 0.4%, the undrained secant stiffness of soils with erosion is larger than that without erosion at the same axial strain. Meanwhile, the undrained peak strength and residual strength are larger for soils with erosion than that for soils without erosion. The less amount of excess pore -water pressure is generated during the undrained compression for the eroded soils comparing to those of the uneroded soils. Furthermore, the eroded soils show a wider instability zone than that of the uneroded soils, which suggests that the instability zone be enlarged by the internal erosion. Besides, one-dimensional upward seepage tests were performed to investigate the change of fabric of the mixed sand with 15%, 25%, and 35% fines contents due to internal erosion. The recorded microscopic images of soils before and after erosion reveal that the fabric is altered by the internal erosion.

Key words: fines content, internal erosion, undrained compression, soil strength

Introduction

Internal erosion is a subsequent transport of detached finer soil particles through the matrix under seepage flow. The initiation of internal erosion has been investigated in terms of the susceptibility of material, hydraulics, and mechanics (Bonelli 2012). However, there were only few researches on the mechanical consequences of soil subjected to internal erosion from the viewpoint of fabric (Moffat and Fannin 2011; Moffat et al. 2011). The fabric here represents the composition of soil, the spatial arrangement of particles, particle groups, and pore spaces (Mitchell and Soga 2005). This fabric may be affected by fines content and specimen preparation method for the soil testing on reconstituted specimens.

Internal erosion causes physical and mechanical changes in soil in many ways. Ke and Takahashi (2012, 2014b) conducted seepage tests in a column and a triaxial permeameter, respectively, and observed that internal erosion would trigger the deformation of tested soils and consequently result in the alteration of soil strength. Moreover, that amounts of deformation and soil strength change were related with the assigned hydraulic conditions (i.e., imposed hydraulic gradient or Darcy velocity). Coincident with the experimental investigations, several novel models for internal erosion had been proposed. Based on the laboratory experiments performed by Sterpi (2003), the empirical law had been derived to describe the process of erosion, in which the amount of eroded soil was considered as a function of time and of the hydraulic gradient. By adopting that erosion law, Cividini and Gioda (2004) proposed a finite element approach in analyzing the transportation of fines. To estimate the quantity of eroded soil mass induced by internal erosion and the resulting settlement of shallows foundations in the city of Milan, Cividini et al. (2009) improved that erosion law in the rate form, and accordingly performed finite element simulations. It was indicated that the erodible fines showed an upper limit diameter of 0.074 mm. The transportation of these fines by seepage flow led to a decline in soil density and a settlement of nearby buildings. Besides, the multi-scale approaches were applied to simulate the process of internal erosion and to examine the mechanical consequences by Scholtès et al. (2010). It was elaborated that the internal erosion tended to increase the porosity, which led to a decrease of the angle of shearing resistance. Muir Wood et al. (2010) simulated internal erosion by discrete element method (DEM) and concluded that the change of the grading by the extraction of fines would cause a change of the critical state in the effective stress plane, resulting in a change of soil strength.

Figure 1 shows the schematic diagram of typical behaviors of granular soils in the undrained compression test. Here the shear stress is defined as the difference between the axial and radial stresses. The undrained peak state (A and A' in Fig. 1) is a state where shear stress reaches an initial local maximum value in the stress–strain curve, quasi-steady state (B and B' in Fig. 1) is where the shear stress reaches a minimum value (Alarcon-Guzman et al. 1988). Phase transformation state (C in Fig. 1) is an indication that soil behavior changes from contractive to dilative. The points D and D' stand for the critical state, which represents the ultimate condition where the plastic shearing could continue indefinitely without changes in volume or effective stress (Muir Wood 1990). When the critical state coincides with the quasi-steady state, it indicates the occurrence of flow behavior (dashed line in Fig. 1) (Tsukamoto et al. 2009). The limited flow behavior (solid line in Fig. 1) suggests that the shear stress temporarily decreases after its initial peak, but reaches a larger value at critical state as shearing continues.

Many experiments have been performed on soil mixtures to examine the effects of fines content on the soil mechanical behavior. Thevanayagam and Mohan (2000) reported that the shear stress at undrained peak state was smaller for the soil with plastic fines than that for the clean sand at the same void ratio when the fines content was smaller than 30%. The shear stress at undrained peak state decreased with an increase in nonplastic fines for Lagunillas sand and Tia Juana sand (Ishihara 1993). Murthy et al.

(2007) indicated that the Ottawa sand with nonplastic fines (5%, 10%, and 15%) showed a more contractive and collapse tendency. Nevada sand with nonplastic fines content (10%, 20%, and 30%) also showed a more contractive behavior than the clean sand in both drained and undrained monotonic compression test (Lade and Yamamuro 1997). Meanwhile, Nevada sand with 7% nonplastic fines showed flow behavior and limited flow behavior at relative small initial confining pressure (Yamamuro and Covert 2001). A reduction of shear stress at the quasi-steady state caused by an addition of plastic fines (10% and 20%) was reported by Ni et al. (2004). The instability zone became larger with the increase in plastic fines content up to 10%, whereas it decreased when the fines content was greater than 20% (Abedi and Yasrobi 2010). Here the instability zone is defined as the zone between the line connecting the origin to the undrained peak state and the line connecting the origin to the phase transformation state in the effective stress plane for cohesionless soil.

The influence of fines on critical state has been widely studied. Murthy et al. (2007) noted that an addition of nonplastic fines led to an increase in the angle of shearing resistance. The shear stress at an axial strain level of 20%–25% decreased with an addition of nonplastic fines to clean Nevada sand (Thevanayagam, 1998). Ni et al. (2004) manifested that the position of the critical state line (CSL) of the soil mixture containing plastic fines in the void ratio and mean effective stress plane was greatly influenced by the stress history, whereas the position of the CSL in the same plane of the soil mixture containing nonplastic fines was mostly affected by the soil fabric comparing to the stress history. Rahman et al. (2011) reported that the CSL in the void ratio and mean effective stress plane shifted downward with an addition of nonplastic fines within the range of threshold fines content. However, when the fines content was beyond the threshold value, the CSL moved upward with the increase of fines content.

The undrained behavior is influenced by the soil preparation method as well. It was observed that the soil prepared by moist tamping method showed a more contractive behavior than that prepared by water pluviation (Vaid et al. 1990). Yang et al. (2008) noted that the dilative responses dominated for the soil prepared by moist tamping method comparing to that prepared by dry deposition method.

This paper describes the results of a laboratory study of undrained behavior of soils with and without erosion. The focus is to examine the difference of overall undrained behavior at both small strain level and large strain level of eroded soils and uneroded soils. The undrained peak state is discussed in terms of peak strength and mean effective stress ratio. Besides, the initial secant stiffness is illustrated. Changes induced by the internal erosion at quasi-steady state and phase transformation state are elaborated by interpreting the variance in residual strength and flow potential. The possible reasons for the changes of the behavior of soils with erosion are demonstrated by the microscopic observation of the soils before and after the internal erosion. Finally, the correlation between the undrained peak state and the quasi-steady state, together with that between undrained peak state and the phase transformation state, is demonstrated.

Experimental program

Tested materials

All the materials in the experiments were mixture of silica No. 3 and No. 8. Individual particle is subround to subangular in shape and predominant mineral is silica. Silica No. 3 is regarded as coarse particles, which forms the skeleton of the specimen. Silica No. 8 is treated as fines, which could be transported by seepage flow. The properties of the individual sand and the mixed sands with 15%, 25%, and 35% fines contents are shown in Table 1, and the particle-size distribution curves are plotted in Fig. 2. One group of tested specimens was prepared with initial fines contents of 0, 15%, 25%, and 35% by weight. The undrained monotonic compression tests were performed on this group to examine the influence of initial fines content on the undrained mechanical behavior. Another group of tested specimens was prepared with 15%, 25%, and 35% initial fines contents, on which the seepage tests and subsequent undrained compression tests were performed to investigate the effects of internal erosion on soil behavior. The seepage tests performed on this group of specimens were carried out in a revised triaxial cell developed by Ke and Takahashi (2014a), which is shown in Fig. 3.

Test apparatus

The main part of the triaxial apparatus is summarized here. The vertical axial load was automatically applied by the loading system with a motor-gear system, which could compress the tested specimen at a given strain rate. The cell pressure was applied by the regulated air pressure whose source was maintained constantly at 700 kPa through an automatic air compressor. A 5 mm thickness mesh with 1 mm openings, which follows the recommendation from the U.S. Department of Agriculture (USDA 1994) to fully hold the coarse particles and allow the erosion of fines, was placed on the end-platen of the pedestal. The base pedestal was revised to accommodate the seepage tests. The drilled conical trough and the tube directly connecting the conical trough with the sedimentation tank were designed to allow the fully dislodgement of fines from the specimens. A miniature load cell in the sedimentation tank would record the cumulative eroded soil mass during the seepage test.

Test procedures

All the specimens were prepared targeting the same initial relative density (Dr = 30%). The size of the soil specimens was approximately 70 mm in diameter and 150 mm in height. The moist tamping method was employed in this study. If each layer is compacted to the target density, the lower portion of the specimen becomes denser than the upper portion because the repeated compaction energy is applied to the lower portion with succeeding compaction. To avoid this problem, other than the final layer, each layer was compacted to a lower density than the target density of the whole specimen according to the undercompaction theory (Ladd 1978). This study adopted Lade's undercompaction theory, and the soil specimen has been prepared layer by layer with 10 layers in total. To guarantee the target soil density is actually achieved, the after-test oven-dry weight of the soil specimen has been checked.

After the soil preparation, the top cap was attached and fixed on the surface of the specimen. The vacuum saturation procedure (JGS 2000; ASTM 2012) was adopted in the experiment. Vacuum was applied to the specimen through water reservoirs gradually until –80 kPa, keeping the pressure difference inside and outside of the specimen constant at 20 kPa. The de-aired water with a total volume of about 10 times of the pore volume was slowly injected into the specimens from the bottom. Generally, the B value of these specimens equals to or is greater than 0.95, which was considered as saturated specimens in this test. After the saturation, all specimens were isotropically consolidated by an automatic control system to an initial mean effective stress of 50 kPa.

The undrained monotonic compression test was performed on one group of specimens containing 0, 15%, 25%, and 35% fines contents with an axial strain rate of 0.1%/min (JGS 2000; ASTM 2012) upon the completion of consolidation to examine the influence of fines content on the undrained behavior.

To study the influence of internal erosion on the soil mechanical behavior, seepage test was performed on the other group of specimens in the triaxial cell after the complete isotropic consolidation. The water in the seepage tests was supplied by the water reservoir shown in Fig. 3, and it was pumped into the specimens by the flow pump. The procedure of the application of flow rate is shown in Fig. 4, which is the same as the test conducted by Ke and Takahashi (2014a). At first, the seepage flow was assigned at a relatively lower flow rate. Then a constant large flow rate (5.2×10^{-6} m^3/s) was applied to the specimen. Upon the completion of the seepage test, the undrained monotonic compression test was performed on the eroded soils with an axial strain rate of 0.1%/min (JGS 2000; ASTM 2012).

Test results

Seepage test results

According to Kenney and Lau (1985), the particles finer than grain size d would likely to be eroded from a soil matrix if there were fewer particles in the grain sizes from d to 4d. In this study, the mixtures of silica No. 3 and No. 8 were gap-graded soils. Therefore, part of fines would be transported by the assigned seepage flow and accumulated in the sedimentation tank (Fig. 3). A summary of results of seepage tests is shown in Table 2. To show the repeatability of test results, seepage tests and subsequent undrained compression tests were carried out twice on the soils with 25% initial fines content, corresponding to the specimens 25_WE_DR30_N1 and 25_WE_DR30_N2 (where the first number in the specimen ID represents percentage of fines content; the second entry is with or without erosion; the third is relative density percentage; and the fourth is test number). The evolutions of the cumulative eroded soil mass are shown in Fig. 5. It is noted that the fines are eroded away from the specimen continuously at the constant flow rate. As the seepage tests were performed on gap-graded soils under isotropic stress state, it could be assumed that the effective stresses are mainly transferred by the coarse fractions. Therefore, the intergranular void ratio, defined by regarding the fines as voids, is considered as one of the parameters in interpreting the relation between initial fines content and cumulative eroded soil mass. Observations of Table 2 reveal that the intergranular void ratios are similar for specimens with 15% and 25% initial fines contents before and after seepages tests whilst the specimen with 35% initial fines content shows a reduction of intergranular void ratio after erosion. It suggests that the fines in these mixtures might not be involved in the stress transformation, which then results in easier transportation of fines when subjected to certain seepage flow. Therefore, it could be concluded that the more the initial fines content, the larger the amount of cumulative eroded soil mass within the scope of this study.

The median particle size of coarse and fine particle is 1.76 and 1.16 mm (Table 1), respectively. If both are assumed as spheres, the diameter of the inscribed sphere in the minimum void space formed by coarse particles is around 0.73 mm. It is approximately five times larger than the median diameter of fines, which suggests a smaller possibility of the occurrence of clogging of fines. Thus the increase in the initial fines content does not necessarily reduce the cumulative eroded soil.

The soil particles were transported by the water flow, which results in a change of volumetric strain during the seepage tests. Figure 6 shows the evolution of the volumetric strain during the seepage tests. There are many jumps in the volumetric strain change for the soil with 35% fines content, which might be attributed to the sudden erosion of the fines by seepage flow. It is indicated that the volumetric strain change is related to the initial fines content. The volumetric strain of the soil with 35% initial fines content (35_WE_DR30) is approximately five times larger than the soil with 25% initial fines content (25_WE_DR30_N1) at the end of the test.

Undrained compression test results

A summary of test results of the undrained compression test of soils without erosion is shown in Table 3. The relationships between the shear stress and the axial strain for the undrained compression tests on the soils without erosion are shown in Fig. 7 and the corresponding effective stress paths are plotted in Fig. 8. It can be seen that the uneroded soil with 35% fines content (35_WOE_DR30) shows the flow behavior, whereas those with 15% and 25% fines contents (15_WOE_DR30, 25_WOE_DR30) shows the limited flow behavior. These indicate that the undrained mechanical behavior of the soil is influenced by the fines content and the soil becomes contractive with the increase of fines in this study.

Table 4 shows the undrained compression test results of soils with erosion, including the maximum hydraulic gradient. It can be observed that all the maximum hydraulic gradients are larger than 1.0, which is considered in the experiments to remove the majority of fines from the specimen. The hydraulic gradient of the specimen with 35% initial fines content (35_WE_DR30) showed the largest hydraulic gradient. It might be responsible for this mixture containing the largest amount of initial fines, which then leads to the smallest hydraulic conductivity.

Figure 9 shows the stress–strain relationships of soils with erosion. All the specimens having experienced internal erosion show a limited flow behavior. The effective stress paths of the soils with erosion are plotted in Fig. 10. It can be observed that all the eroded specimens show dilative tendency, i.e., the mean effective stress increases after passing through the phase transformation state.

The particle size analysis performed after compression tests reveal that the eroded specimens are not homogeneous, which might be responsible for the occurrence of erosion in preferential flow paths. It is considered as the inherent consequences of seepage tests.

Microscopic observation

Due to the limitation of laboratory test condition, the microscopic observation was performed at the upward seepage tests to describe the changes of particles structure induced by internal erosion. The mixtures with 15%, 25%, and 35% initial fines contents were prepared targeting a relative density of

30%. The moist tamping method was employed to create the similar soil fabric as that in the triaxial tests. Figure 11 shows the schematic diagram of the upward seepage test apparatus. The apparatus mainly consists of a rectangular seepage cell with a transparent glass window in front and a water reservoir. The internal dimensions of the rectangular seepage cell are 130 mm in height, 100 mm in length, and 30 mm in width. A 30 mm in thickness gravel diffusing filter was put to ensure a uniform flow across the specimens within a reasonable range. The size of the specimens is 60, 100, and 30 mm in height, length, and width, respectively.

After the preparation of specimens, a vertical stress of 50 kPa was applied to the soils to simulate the stress level in the triaxial cell under consolidation. The upward seepage flow was then applied from the bottom of the specimens after removing the vertical stress. The main objective of this test is to observe the change of soil microstructure, thus the influence of stress state is not considered at this point. The inlet flow was provided by the water reservoir, which can be raised or lowered to control its water head difference with the top of the specimens. The discharge rate was measured by the cylinder placed at the outlet from the basin. The applied maximum hydraulic gradient was large enough to dislodge most of the unstable fines away from the specimens by the assigned upward flow. In this study, the maximum applied hydraulic gradient is over 1.0.

A digital microscope with a resolution of about 1000 units × 1000 units was used to observe the distributions of fines and coarse particles during the seepage tests. The lens of the microscope was placed in front of the transparent glass window, as shown in Fig. 11.

It is well recognized that if clean sand is mixed with fines, soil microstructure will change as a consequence and that change somehow corresponds to the amount of fines content (Yamamuro and Covert 2001). An observation of the evolution of the microstructure of silica No. 3 with the increasing content of silica No. 8 (i.e., 0, 15%, 25%, and 35%), regarding as fines, is presented in Fig. 12. All those moist tamped specimens have the initial relative density of 30%. Initially, without the presence of fines, the contacts between coarse particles are well developed. With the introduction of small amounts of fines (i.e., 15%), the coarse particles are coated by the fines and a fraction of fines fills the voids between coarse particles. In terms of the specimen with large amounts of fines (i.e., 25%), the dominant contact network of coarse particles might be partially destroyed, leading to more occurrence of separation of coarse particles by fine fractions. When it comes to a larger fines content (i.e., 35%), the voids between coarse particles are almost occupied by fines.

Skempton and Brogan (1994) postulated that the fines having filled the voids do not take part in the load transfer, therefore, it is expected they would be easily dislodged by the upward seepage flow. The images collected upon the completion of internal erosion (Fig. 13) proved this postulation. It is indicated that most of the fines occupying the voids formed by coarse particles were moved away by fluid flow. Although the results of upward seepage tests cannot be quantitatively compared to the downward seepage tests, they could be qualitatively correlated. For instance, fines were eroded away from specimens; hydraulic gradient and hydraulic conductivity changed; void ratios and volume of specimens were altered with the progress of internal erosion. Interestingly, at some spots, due to the small constriction size of voids, amounts of fines were impeded and consequently accumulated around the contact points of coarse particles, forming the jamming fines. Those fines would actively participate in the load transfer. Microscopically, these jammed fines may be involved in the load transfer and macroscopically they would result in different undrained responses from the soils without erosion, which will be discussed in detail later.

Albeit different, the flow direction is compared to triaxial seepage tests, the inherent mechanism of internal erosion being the same, i.e., process of fines transport. It is also argued that the fabric observed through the transparent window could be different from the inside of the specimen, which might be considered as an inherent limitation for the upward seepage tests. Although the images recorded in the front of the transparent window might exaggerate the phenomenon of internal erosion, the evolutions of soil microstructure could also be presented, which is the very purpose of the upward seepage tests. Therefore, the images recorded from these tests are utilized as supplemental evidences in discussing soil mechanical behaviors in triaxial tests.

Discussions

Detailed examination of the undrained mechanical behavior can help to get a throughout understanding of the influence of fabric on soil behavior. The undrained characteristics of soil behavior at the undrained peak state, quasi-steady state, phase transformation state, and critical state are discussed in order, followed by an interpretation based on the soil fabric. The relations between the key states are presented as well.

Undrained Peak State

Undrained peak strength

The undrained peak state is the state where the shear stress reaches the initial peak in the stress–strain curve in the undrained monotonic compression test. It is associated with the onset of the flow failure (Yoshimine and Ishihara 1998). One of the soil strength parameters related to the undrained peak state is the undrained peak strength (s_p) (Ishihara 1993), which is customarily defined as

(1)
$$s_p = \frac{q_{ups}}{2}$$

where q_{ups} is the shear stress at the undrained peak state. Figure 14 shows the relationship between the undrained peak strength normalized by initial mean effective stress and the fines content before compression. It is found that the uneroded soil with 15% initial fines content (15_WOE_DR30) shows larger normalized peak strength than those with 25% and 35% initial fines contents (25_WOE_DR30, 35_WOE_DR30). Besides, it can be observed that the eroded soils show the larger peak strength than those of the uneroded soils with the same initial fines contents although the void ratio of the eroded soils becomes larger due to the internal erosion. Take the soils with 15% initial fines content for example, the uneroded specimen (15_WOE_DR30) shows normalized peak strength of 0.63, whereas the eroded specimen (15_WE_DR30) shows normalized peak strength of 0.85. Moreover, it can be found that the normalized peak strength of the soils with erosion is not located in the same band compared with the soils without erosion. The normalized peak strength of soils with erosion seems to be sensitive to the fines content before compression. The normalized peak strength of the soils with erosion shows different values from 0.28 to 0.85, although they contain similar fines contents around 10% (ranging between 9% and 13%).

Mean effective stress ratio

Another important parameter at the undrained peak state is the mean effective stress ratio, which is defined as the value of mean effective stress at undrained peak state (p'_{ups}) divided by initial mean effective stress (p'_0) (Ishihara 1993). Figure 15 shows the mean effective stress ratio at the undrained peak state against fines content before compression.

Information about the reference data is shown in Table 5. These data are taken from the previous works on loose sands mixed with fines, prepared by the moist tamping method. It can be observed that the mean effective stress ratio is greatly influenced by the properties of tests materials. The reference data, soils with 35% initial fines content (35_WOE_DR30, 35_WE_DR30), and uneroded soil with 25% initial fines content (25_WOE_DR30) are located in the same band (i.e., the mean effective stress ratio in between 0.5 and 0.7, irrespective to the fines content before compression). However, the mean effective stress ratios of the soils with 15% initial fines content (15_WOE_DR30, 15_WE_DR30) and the eroded soils with 25% initial fines contents (25_WE_DR30_N1, 25_WE_DR30_N2) are located well above the band. Although the marked difference cannot be seen in the case of the eroded soil with 35% initial fines content, the mean effective stress ratios of soils with erosion are relatively larger than the soils without erosion.

Undrained secant stiffness

It is generally accepted that soil behaves nonlinearly even at a relative small strain level. Undrained secant stiffness at an axial strain in the range of 0.1%–1% is very useful in interpreting the soil behavior at initial shearing stage. Figure 16a shows the undrained secant stiffness of soils without erosion. The undrained secant stiffness here is normalized with initial mean effective stress and is plotted against the axial strain. The similar plots for the eroded soils are shown in Fig. 16b. It should be noted that the uneroded soil with 15% initial fines content (15_WOE_DR30) shows larger normalized secant stiffness than those with 25% and 35% initial fines contents (25_WOE_DR30, 35_WOE_DR30) when the axial strain is less than 0.9%. That is to say, the soil with smaller initial fines content indicates the larger shear stiffness than those with larger initial fines content at a small strain level. From Fig. 16b, it can be observed that for the specimens with the same initial fines content, the post-erosion soil exhibits larger normalized secant stiffness compared to that without erosion when its axial strain is less than 0.4%. Take the specimens with 15% initial fines content at 0.25% axial strain for instance, the uneroded soil shows a normalized secant stiffness of 200, whereas the eroded soil shows a normalized secant stiffness of 230.

Quasi-steady state

Another key state of the undrained behavior is the quasi-steady state where the shear stress shows a local minimum value in the stress–strain curve. The quasi-steady state appears only when the metastable specimens exhibit the strain softening behavior during the undrained compression. The soil shows a minimum shear stress at the quasi-steady state, which can be even smaller than that at critical state where the soil is sheared to a relatively larger strain. Residual strength, which is associated with the shear stress at quasi-steady state, is recommended to use in stability analyses by Sladen et al. (1985). They reported that the application of residual strength could be considered valid when the soil strength is believed to be affected by some factors. Thus, it would be safer if the residual strength is taken into consideration in analyzing the soil experienced with internal erosion.

The residual strength (s_{us}) at the quasi-steady state is customarily defined as

$$s_{us} = \frac{q_{qss}}{2}\cos\phi_s = \frac{M_{qss}}{2}\cos\phi_s\,(p'_{qss}) \tag{2}$$

$$M_{qss} = \frac{6\sin\phi_s}{3-\sin\phi_s} \tag{3}$$

where q_{qss} is the shear stress at the quasi-steady state, ϕ_s is angle of shearing resistance at quasi-steady state, p'_{qss} is the mean effective stress at the quasi-steady state, and M_{qss} is the shear stress ratio at the quasi-steady state (q_{qss}/p'_{qss}). It can be observed from Figs. 7 and 9 that all of the mixed sands with initial fines contents of 15%, 25%, and 35% show strain softening behavior after the initial peak in the stress–strain curves. Therefore, it can be said that the quasi-steady state appears for these specimens in this study.

Figure 17 shows the shear stress ratios at the quasi-steady state against fines content before compression on the soils with and without erosion. It is noted that the stress ratios of soils without erosion almost stay in a narrow brand of 1.30, corresponding to an angle of shearing resistance of 32.2°

at the quasi-steady state, irrespective of the fines content before compression. However, the shear stress ratio of soils with erosion is not a constant value and fluctuates around 1.30. This deviation from the band may suggest that the shear stress ratio at quasi-steady state also be influenced by the internal erosion.

The normalized residual strength with initial mean effective stress against fines content before compression is shown in Fig. 18. The normalized residual strengths of mixed Hokksund sand and Chengbei silt from Yang et al. (2006b) are also plotted in this figure. These mixed soils were prepared by moist tamping method with fines contents of 0, 5%, 10%, 15%, 20%, 30%, and 50%, targeting a relative density ranging from 22% to 30%. It can be observed from Fig. 18 that the normalized residual strength is affected by fines content. For the silica sand in this study, the specimens with larger fines content before compression show a smaller normalized residual strength. The normalized residual strength change with the fines content before compression in this study shows the similar tendency as the mixtures of Hokksund sand and Chengbei silt (Yang et al. 2006b).

Meanwhile, the soils with erosion show a larger normalized residual strength than the soils without erosion at the same initial fines content as for the normalized peak strength in this study. For example, at the same initial fines content of 15%, the soil without erosion shows a normalized residual strength of 0.41, but the soil with erosion shows a normalized residual strength of 0.63. This fact suggests that the soils become less contractive when they experience internal erosion.

Phase transformation state

Phase transformation state is the state where the soil shows a minimum mean effective stress in the effective stress path (Ishihara et al. 1975). It is also an indication that the soil changes from contractive behavior to dilative behavior. In many cases the phase transformation state is coincident with the quasi-steady state although the definitions of these two states is different, i.e., the former is defined by the minimum mean effective stress and the latter is defined by the minimum shear stress. Typically, the quasi-steady state precedes the phase transformation state in the monotonic undrained compression.

The phase transformation state is one of the key states associated with the potential of flow failure because the value of excess pore-water pressure during compression is the maximum in this state. The flow potential (u_f) proposed by Yoshimine and Ishihara (1998) represents the maximum excess pore-water pressure ratio during the undrained monotonic compression test, and is expressed as

$$u_f = (1 - \frac{p'_{pts}}{p'_0}) \times 100\% \qquad (4)$$

where p'_{pts} is the mean effective stress at the phase transformation state, and p'_0 is the initial mean effective stress. The value of flow potential varies from 0 to 100%. The soil with a small value of u_f means that it generates a small amount of excess pore-water pressure under the undrained compression.

The relationship between flow potential (u_f) and fines content before compression is shown in Fig. 19. Information about the reference data is shown in Table 5. It can be seen that the uneroded soils with 15%, 25%, and 35% fines contents indicate a flow potential (u_f) ranging from 33% to 92% in this study. The flow potential is very sensitive to the fines content in the undrained compression test. In this study, the silica sand with a larger fines content before compression shows a larger flow potential than that with less fines content. The Nerlerk sand (Sladen et al. 1985) and Ottawa sand (Murthy et al. 2007) shown in Fig. 19 indicated the same tendency. That is to say, the potential of flow failure is considered higher for the soil containing a larger amount of fines.

One of the other observations from Fig. 19 is that the flow potential (u_f) of soils with erosion is smaller than that of soils without erosion at the same initial fines content. Taking the soils with 15% initial fines content for example, the flow potential (u_f) of soil without erosion (15_WOE_DR30) is 33%, whereas that of soil with erosion (15_WE_DR30) decreases to 0.5%. In addition, the slopes of the relationship between the fines content before compression and flow potential are more or less the same for the soils without erosion as indicated in the dash lines, while it is steeper for the eroded soil (dotted line in Fig. 19). This difference indicates that the compressibility of the eroded soil is more sensitive to the fines content compared to the uneroded soils.

Critical state

The concept of critical state is an effective and useful framework for discussing the soil behavior, which is defined as the state where the soils continue to deform without change of effective stress or migration of pore water (Roscoe et al. 1958). The pioneer study on the evolution of CSL with erosion is presented by Muir Wood (2007) by adopting the concept of "grading state index". In their approach, "grading state index" is defined as the ratio of the current grading to the limiting grading, which varies from 0 to 1 corresponding to the changes from single sized grading to certain limiting grading. The direct consequences of internal erosion include the movement of particle grading curve due to the amounts of fines loss, which accordingly changes the grading state index. Figure 20 indicates the movement of particle grading curves of the tested specimens (25_WOE_DR30, 25_WE_DR30_N2) induced by internal erosion. Coincident with the studies of Muir Wood and Maeda (2008) and Muir Wood et al. (2010), the grading curve moves downward after internal erosion and the extent of that movement may represent the amounts of fines loss, suggesting a decline in grading state index. Further, it may cause the upward movement of CSL in the *e-log p'* plane.

In this study, the undrained test data were interpreted to understand the corresponding evolution of

CSL with internal erosion. For those cases without sufficient straining, a sigmoidal function fitting proposed by Murthy et al. (2007) was utilized to extrapolate the critical state, the details of which are explained in Appendix A. Figure 21 shows the critical state of soils before and after erosion. The CSL of the uneroded specimens with 35% fines content was derived from the results of the laboratory compression tests. Unfortunately, similar tests on the specimens with 15% and 25% fines contents have not been performed. Therefore, the CSLs of soils with 15% and 25% fines contents, shown in Fig. 21, were postulated on the basis that the soil with a smaller fines content shows a steeper CSL in the *e-log p'* plane (Murthy et al. 2007). Zlativoc and Ishihara (1997) concluded that critical state may erase the influence of initial fabric and in this circumstance the soil mechanical responses tend to become similar. It is noted from Table 4 that the fines contents of eroded specimens before compression are similar, ranging from 9% to 13%. Therefore, it can be assumed that the critical states of the eroded specimens somehow locate on a similar CSL, which is above that of the uneroded specimens. The movement of CSL is in accordance with the theoretical prediction of Muir Wood and Maeda (2008) and Muir Wood et al. (2010): due to the decrease of grading state index induced by internal erosion the CSL in the *e-log p'* plane moves upwardly.

Effects of fines content on undrained behavior

As shown in the previous subsections, the uneroded specimens containing a smaller amount of fines show a larger value of peak strength, undrained secant stiffness, and residual strength than that containing a larger amount of fines. These undrained behaviors on the soils without erosion may be affected by the soil fabric.

All the specimens in this study were prepared by moist tamping method. It is well known that the moist tamping method would create metastable honeycomb structures among coarse particles. The images in

Fig. 12 taken by a digital microscope reveal the micro soil fabric to some extent in this study. The honeycomb structure can be clearly observed in the soil with 15% fines content because the voids between coarse particles are hardly filled with fines. However, in the soil with 25% fines content, the voids between coarse particles are partially filled with fines. In the soil with 35% fines content, these voids are largely filled with fines. Most of the coarse grains seem to be floating on the fines. Therefore, the honeycomb structure cannot be obviously observed in the soils with 25% and 35% fines contents.

Observations of the contacts in the binary soil mixtures are formed randomly by fines and coarse particles. The fines in between the coarse particles in the soil with 15% fines content are less than those in the soils with 25% and 35% fines contents. It might be possible to assume that the amount of the jamming fines is less in the soil with 15% fines content. According to Salgado et al. (2000), during compression, the coarse particles may be easily moved side away for the soil with less jamming fines (i.e., soil with 15% fines content), leading to greater direct contacts between coarse particles during shearing. The load may be more efficiently transferred through the coarse particles than through the fines. Therefore, it is possible to deduce that the uneroded soil with smaller fines content would show a relatively larger peak and residual strength than that with larger fines content within the test range.

Summary of effects of internal erosion on undrained behavior

Through the comparison between the soils with and without erosion, it is noted that the undrained behavior of the eroded soils is different from that of the uneroded soils. The soils with erosion show a larger peak and residual strength that those without erosion, which probably means that the soils become less contractive after internal erosion. One of the reasons for the dilative behavior of soils with erosion might be the dilative characteristic of silica No. 3. As indicated in Figs. 7 and 8, the specimens made of silica No. 3 only show a fully dilative behavior in the undrained compression test even at loose condition (initial relative density of 20% and 30%).

The soils with erosion have similar fines content before compression, but they showed different behavior during the undrained compression tests. For instance, the flow potential of eroded soils shows a wide range of value within only a small range of fines content. Therefore, it could be said that the reason of the difference in the undrained behavior of soils with and without erosion is caused not only by the decrease of fines content because of internal erosion, but also by the change of the fabric. In this study, the soil fabric is observed by digital microscope and the collected images of soils subjected to internal erosion can be seen in Fig. 13.

The coarse particles of the soils with erosion were rearranged due to the internal erosion. The transportation of fines leads to an increase of void space. The hydraulic force induced by the seepage flow not only transports the fines, but also changes the position of the coarse particles, which may have resulted in a fabric that is different from the soils without erosion. This probably changes the way of load transferring in the soils with erosion compared with the soils without erosion.

The contacts between particles may also have been changed by the internal erosion. It can be observed in Fig. 13 that some fines still stay in between the coarse particles after the seepage test. During the progress of the seepage flow, the fines were jammed in the slaps around the contact points between the coarse particles. Thus, the number of the effective contact points increases due to the internal erosion, resulting in a much more efficient transformation of the internal forces.

Relation between key states

The soils used in this study show a local maximum shear stress at the undrained peak state and a minimum shear stress at the quasi-steady state. The local minimum mean effective stress appears at the phase transformation state. The relationships between these states are compared below.

Undrained peak state and quasi-steady state

The tested specimens mostly exhibit initial peak strength followed by a local minimum in the stress–strain curve, which corresponds to the residual strength at the quasi-steady state. The relationship of the shear stress normalized by the initial mean effective stress between the undrained peak state and quasi-steady state is shown in Fig. 22. According to the definition of the undrained peak state and quasi-steady state, the shear stress at the former state would always be larger or equal to that at the latter state. To show the relationship clearly, a demarcation line where the shear stress at undrained peak state equals to that at quasi-steady state is also drawn as the solid line in Fig. 22. If the difference between the normalized peak strength and normalized residual strength is small, the state point is located around the demarcation line, suggesting a less contractive behavior. For example, the specimens 25_WOE_DR30_N1 and 25_WE_DR30_N2 show a relatively less contractive behavior, so their states locate very near the demarcation line. It can be noted that, by comparing the relative position of the points to the demarcation line, the points for the eroded soils are closer to the demarcation line, suggesting a less contractive response.

Undrained peak state and phase transformation state

The undrained peak state is associated with the onset of flow failure, and the phase transformation state is the state where soil behavior changes from contractive to dilative. Between these two states, a relatively small load might be sufficient to cause a large deformation of soil structure. That is to say, the soil would experience an instability state between the undrained peaks state and phase transformation state (Leong and Chu 2002).

The instability line is defined as the line connecting points of the shear stress at the undrained peak state in the effective stress plane. Yang et al. (2006a) found that the instability line passes through the origin in the effective stress plane for the cohessionless soils. Therefore, the instability line here is described as the line connecting the origin to the point at the undrained peak state in the effective stress path. The instability zone is defined as the zone between the instability line and the line connecting the origin to the phase transformation state in the effective stress plane.

The normalized slope differences against the fines content before compression are shown in Fig. 23. The normalized slope difference here is defined as the difference between the slope of the line connecting the origin to the phase transformation state and that of the instability line in the effective stress plane, normalized by the slope of the line connecting the origin to the phase transformation state. It enables to quantitatively evaluate the instability zone: the soil with a larger slope difference indicates a wider instability zone. It is noted that the slope differences of soils with erosion are larger than those of soils without erosion at the same initial fines content, especially for the soil with 25% initial fines content, the slope difference of that without erosion (25_WOE_DR30) is 0.28, whereas the average slope difference of that with erosion (25_WE_DR30_N1, 25_WE_DR30_N2) is 0.48, suggesting that the instability zone is enlarged by the internal erosion. The big change in the slope difference between the eroded soils and uneroded soils might have resulted from the drastic change of its fabric due to internal erosion. Intergranular void ratio assumes that fines function as voids and therefore the volume of fines is considered as voids. Accordingly, if the intergranular void ratios of soils before and after seepage tests are similar, the specimen losing larger volume of fines would have greater deformation to compensate the changes in volumes of voids, which might indicate greater changes of fabric. Table 2 notes that the intergranular void ratios of specimens with 15% and 25% initial fines contents are similar before and after erosion, but more fines are eroded away from the specimen with 25% initial fines content. Therefore, the fabric change of specimen with 25% initial fines content should be greater than that of specimen with 15% initial fines content. This tendency corresponds to a larger change of slope difference for specimen with 25% initial fines content (Fig. 23). In contrast, the intergranular void ratio of the specimen with 35% initial fines content decreases after erosion, which suggests that the coarse fraction is further compacted after internal erosion. Although the specimen with 35% initial fines content shows the largest cumulative eroded soil mass, the balance between the amounts of fines erosion and compaction of coarse fraction leads to less change of its slope difference than that of specimen with 25% initial fines content. Future study on the fabric of soils subjected to internal erosion might be helpful in understanding its mechanic consequences.

Conclusions

Seepage tests and undrained monotonic compression tests were performed to examine the influence of initial fines content on (i) the seepage-induced fabric change and (ii) mechanical consequences of soils subjected to internal erosion. The images of the packing of the soil particles were taken by a digital microscope to observe the fabric change before and after the internal erosion. It is found that the seepage flow not only transports fines away from the specimen, but causes a drastic change in the soil fabric, which results in a totally different undrained mechanical behavior for soils with erosion compared with those without erosion. During the seepage tests, the soil with larger initial fines content shows a larger amount of cumulative eroded soil mass and a larger volumetric strain within the test range.

The images collected before and after internal erosion reveal that the soil fabric is altered by the internal erosion. In the uneroded soil with fines, the coarse particles are coated by fines and the distribution of the fines varies with the fines content. While for the soils with erosion, most of remaining fines are jammed around the contact between coarse particles, which results in an increase of the number of effective contact points.

The amounts of silica No. 8 in the tested mixtures would greatly affect their undrained behavior, resulting in the changes of peak strength and residual strength. Specifically, a smaller content of silica No. 8 would cause a larger peak, residual strength, and correspondingly a smaller flow potential.

The internal erosion may change the soil fabric and further influences the undrained behavior. The mean effective stress ratios (ratio of mean effective stress at peak to that at initial) of soil with erosion show different values from the soil without erosion. For the specimens with the same initial fines content, the post-erosion soil exhibits larger undrained secant stiffness compared to that without erosion at a relatively small axial strain level. The soils with erosion show larger residual strength than those without erosion if their initial fines contents are the same. Meanwhile, the eroded soils generate a smaller amount of excess pore-water pressure than the uneroded soils before reaching the phase transformation state. It is also noted that the slope difference between the line connecting the origin to the transformation state and the instability line in the effective stress plane is larger for the soils with erosion, indicating an enlarged instability zone after internal erosion.

Acknowledgement

Support for the first author is provided by a Monbukagakusho (Ministry of Education, Culture, Sports, Science and Technology, Japan) scholarship for graduate students. This work is financially supported by JSPS KAKENHI Grant No. 25420498. The authors express gratitude to their colleagues at Tokyo Institute of Technology, particularly Ke Lin, for their important contributions.

References

Abedi, M., and Yasrobi, S.S. 2010. Effects of plastic fines on the instability of sand. Soil Dynamics and Earthquake Engineering, 30(3): 61–67.

Alarcon-Guzman, A., Leonards, G., and Chameau, J. 1988. Undrained monotonic and cyclic strength of sands. Journal of Geotechnical Engineering, 114(10): 1089–1109.

ASTM D4767-11. 2012. Standard test method for consolidated undrained triaxial compression test for cohesive soils. Annual book of ASTM standards,Vol.04.08, ASTM International, West Conshohocken.

Bonelli, S. 2012. Erosion of geomaterials. Wiley.

Cividini, A., Bonomi, S., Vignati, G.C., and Gioda, G. 2009. Seepage-induced erosion in granular soil and consequent settlements. International Journal of Geomechanics, 9(4): 187–194.

Cividini, A., and Gioda, G. 2004. Finite-element approach to the erosion and transportation of fine particles in granular soils. International Journal of Geomechanics, 4(3): 191-198.

Ishihara, K., Tatsuoka, F., and Yasuda, S. 1975. Undrained deformation and liquefaction of sand under cyclic stresses. Soils and Foundations. 15(1): 29-44.

Ishihara, K. 1993. Liquefaction and flow failure during earthquakes. Géotechnique, 43(3): 351–451.

JGS 0525-2000. 2000. Method for k0 consolidated-undrained triaxial compression test on soils with pore water pressure measurement. Standards of Japanese Geotechnical Society for Laboratory Shear Tests, Japanese Geotechnical Society: pp. 28-34.

Ke, L., and Takahashi, A. 2012. Strength reduction of cohesionless soil due to internal erosion induced by one-dimensional upward seepage flow. Soils and Foundations, 52(4): 698–711.

Ke, L., and Takahashi, A. 2014a. Triaxial erosion test for evaluation of mechanical consequences of internal erosion. Geotechnical Testing Journal, 37(2): 1–18.

Ke, L., and Takahashi, A. 2014b. Experimental investigations on suffusion characteristics and its mechanical consequences on saturated cohesionless soil. Soils and Foundations, 54(4): 713-730.

Kenney, T.C., and Lau, D. 1985. Internal stability of granular filters. Canadian Geotechnical Journal, 22(2): 215–225.

Ladd, R.S. 1978. Preparing test specimens using undercompaction. Geotechnical Testing Journal, 1(1): 16–23.

Lade, P.V., and Yamamuro, J.A. 1997. Effects of nonplastic fines on static liquefaction of sands. Canadian Geotechnical Journal, 34(6): 918–928.

Leong, W.K., and Chu, J. 2002. Effect of undrained creep on instability behavior of loose sand. Canadian Geotechnical Journal, 39(6): 1399–1405.

Mitchell, J., and Soga, K. 2005. Fundamentals of soil behavior. Wiley.

Moffat, R., and Fannin, R.J. 2011. A hydromechanical relation governing internal stability of cohesionless soil. Canadian Geotechnical Journal, 48(3): 413-424.

Moffat, R., Fannin, R.J., and Garner, S.J. 2011. Spatial and temporal progression of internal erosion in cohesionless soil. Canadian Geotechnical Journal, 48(3): 399-412.

Muir Wood, D. 1990. Soil behaviour and critical state soil mechanics. Cambridge University Press.

Muir Wood, D. 2007. The magic of sands. 20th Bjerrum Lecture, presented in Oslo 25 November 2005. Canadian Geotechnical Journal, 44(11): 1329-1350.

Muir Wood, D., Maeda, K., and Nukudani, E. 2010. Modelling mechanical consequences of erosion. Géotechnique, 60(6): 447–457.

Muri Wood, D., and Maeda, K. 2008. Changing grading of soil: effect on critical states. Acta

Geotechinca, 3(1): 3-14.

Murthy, T.G., Loukidis, D., Carraro, J.A.H., Prezzi, M., and Salgado, R. 2007. Undrained monotonic response of clean and silty sands. Géotechnique, 57(3): 273–288.

Ni, Q., Tan, T.S., Dasari, G.R., and Hight, D.W. 2004. Contribution of fines to the compressive strength of mixed soils. Géotechnique, 54(9): 561–569.

Rahman, M.M., Lo, S.R., and Baki, M.A.L. 2011. Equivalent granular state parameter and undrained behaviour of sandfines mixtures. Acta Geotechnica, 6(4): 183–194.

Rao, S.S. 2009. Engineering optimization: theory and practice. John Wiley & Sons.

Roscoe, K.H., Schofield, A.N., and Wroth, C.P. 1958. On the yielding of soils. Géotechnique, 8(1): 22-52.

Salgado, R., Bandini, P., and Karim, A. 2000. Shear strength and stiffness of silty sand. Journal of Geotechnical and Geoenvironmental Engineering, 126(5):451–462.

Scholtés, L., Hicher, P.Y., and Sibille, L. 2010. Multiscale approaches to describe mechanical responses induced by particle removal in granular materials. Comptes Rendus Mécanique, 338(10-11): 627–638.

Skempton, A.W., and Brogan, J.M. 1994. Experiments on piping in sandy gravels. Géotechnique, 44(3): 449-460.

Sladen, J.A., D'Hollander, R.D., and Krahn, J. 1985. The liquefaction of sands, a collapse surface approach. Canadian Geotechnical Journal, 22(4): 564–578.

Sterpi, D. 2003. Effects of the erosion and transportation of fine particles due to seepage flow. International Journal of Geomechanics, 3(1): 111-122.

Thevanayagam, S. 1998. Effect of fines and confining stress on undrained shear strength of silty sands. Journal of Geotechnical and Geoenvironmental Engineering, 124(6): 479–491.

Thevanayagam, S., and Mohan, S. 2000. Intergranular state variables and stress-strain behaviour of silty sands. Géotechnique, 50(1): 1–23.

Tsukamoto, Y., Ishihara, K., and Kamata, T. 2009. Undrained shear strength of soils under flow deformation. Géotechnique, 59(5): 483–486.

U.S. Department of Agriculture (USDA). 1994. Gradation design of sand and gravel filters. Chapter 26, National engineering handbook, Part 33, Soil Conservation Service, Washington, D.C.

Vaid, Y.P., Chung, E.K.F., and Kuerbis, R.H. 1990. Stress path and steady state. Canadian Geotechnical Journal, 21(1): 1–7.

Yamamuro, J., and Covert, K. 2001. Monotonic and cyclic liquefaction of very loose sands with high silt content. Journal of Geotechnical and Geoenvironmental Engineering, 127(4): 314–324.

Yang, S.L., Sandven, R., and Grande, L. 2006a. Instability of sand silt mixtures. Soil Dynamics and Earthquake Engineering, 26(2-4): 183–190.

Yang, S.L., Sandven, R., and Grande, L. 2006b. Steady-state lines of sand-silt mixtures. Canadian Geotechnical Journal, 43(11): 1213–1219.

Yang, Z.X., Li, X.S., and Yang, Y. 2008. Quantifying and modelling fabric anisotropy of granular soils. Géotechnique, 58(4): 237–248.

Yoshimine, M., and Ishihara, K. 1998. Flow potential of sand during liquefaction. Soils and Foundations, 38(3): 189–198.

Zlativoc, S., and Ishihara, K. 1997. Normalized behavior of very loose non-plastic soils: effects of fabric. Soils and Foundations, 37(4): 47-56.

Table 1. Properties of tested materials

	Silica No. 3	Specimen 15	Specimen 25	Specimen 35	Silica No.8
Fines content (%)	0	15.0	25.0	35.0	100
Maximum void ratio	0.94	0.79	0.77	0.74	1.33
Minimum void ratio	0.65	0.53	0.37	0.36	0.70
Median particle size (mm)	1.76	1.78	1.69	1.54	0.16
Curvature coefficient	0.96	8.69	8.54	0.074	0.99
Uniformity coefficient	1.31	13.0	16.4	19.3	1.05

Table 2. Seepage tests results

Specimen No.	F_c[a] (%)	e_0[b]	e_c[c]	e_{cs}[d]	F_{ce}[e] (%)	e_e[f]	e_{es}[g]	ε_v[h] (%)
15_WE_DR30	15	0.68	0.67	0.96	8.75	0.80	0.98	0.11
25_WE _DR30_N1	25	0.61	0.56	1.08	12.0	0.81	1.06	1.62
25_WE_DR30 _N2	25	0.61	0.54	1.05	13.1	0.81	1.06	2.21
35__DR30_WE	35	0.61	0.59	1.45	13.3	0.99	1.29	10.1

[a]Initial fines content, F_c (%).

[b]Initial void ratio, e_0.

[c]Void ratio after consolidation, e_c.

[d]Intergranular void ratio after consolidation (before seepage test), $e_{cs}=(e_c+F_c/100)/(1-F_c/100)$.

[e]Fines content after seepage test, F_{ce} (%).

[f]Void ratio after seepage test, e_e.

[g]Intergranular void ratio after seepage test, $e_{es}=(e_e+F_{ce}/100)/(1-F_{ce}/100)$.

[h]Volumetric strain, ε_v (%).

Table 3. Undrained compression test results of soils without erosion

Specimen No.	Fines content, F_c (%)	Initial void ratio, e_0	Void ratio after consolidation, e_c	Axial strain at undrained peak state (%)	Axial stain at quasi-steady state (%)	Axial strain at phase transformation state (%)
00_WOE_DR20	0	0.84	0.84	--	--	--
00_WOE_DR30	0	0.82	0.82	--	--	--
15_WOE_DR30	15	0.68	0.67	0.99	3.92	4.58
25_WOE_DR30	25	0.61	0.56	2.27	2.34	3.60
35_WOE_DR30	35	0.60	0.56	0.58	8.11	8.59

Table 4. Undrained compression test results of soils with erosion

Specimen No.	Fines content after seepage test, F_{ce}(%)	Void ratio after consolidation, e_c	Maximum hydraulic gradient, i_{max}	Void ratio after seepage test, e_e	Axial strain at undrained peak state (%)	Axial stain at quasi-steady state (%)	Axial strain at phase transformation sate (%)
15_WE_DR30	8.75	0.67	2.07	0.80	1.00	3.77	4.92
25_WE_DR30_N1	12.0	0.56	5.05	0.81	1.93	3.93	6.59
25_WE_DR30_N2	13.1	0.54	5.39	0.81	2.20	4.64	4.70
35_WE_DR30	13.3	0.59	11.7	0.99	1.07	4.83	6.06

Table 5. Information of reference data

Tested materials	Fines content (%)	Relative density (%)	Preparation method	References
Leighton Buzzard sand, Nerlerk sand	0, 2.2, 12	10 - 30	Moist tamping	Sladen et al. 1985
Toyoura sand	0	7 - 65	Moist tamping	Ishihara 1993
Ottawa sand	0, 5, 10, 15	20 - 50	Moist tamping	Murthy et al. 2007

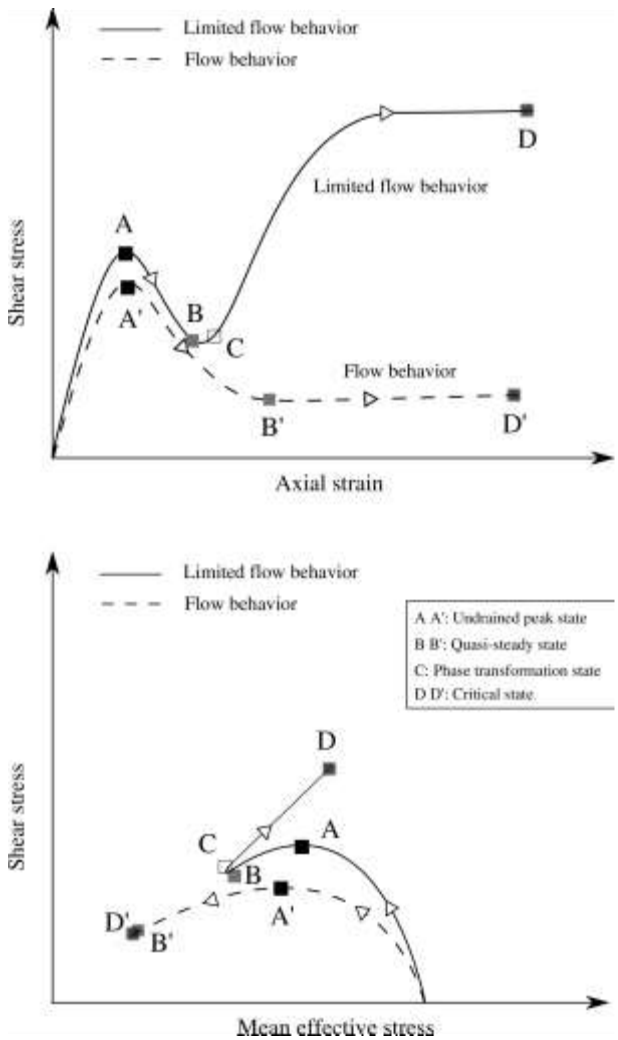

Fig. 1. Schematic diagram of the characteristics of typical undrained behaviors

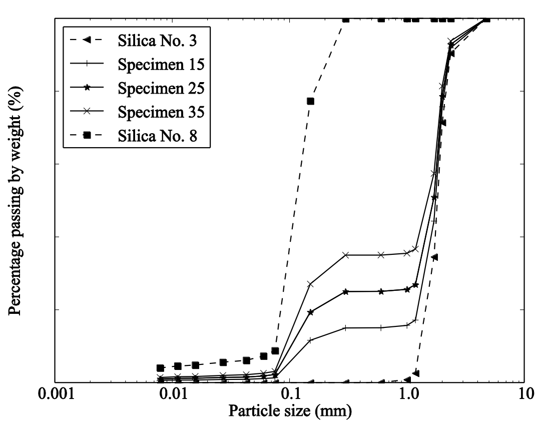

Fig. 2. Particle size distribution curves

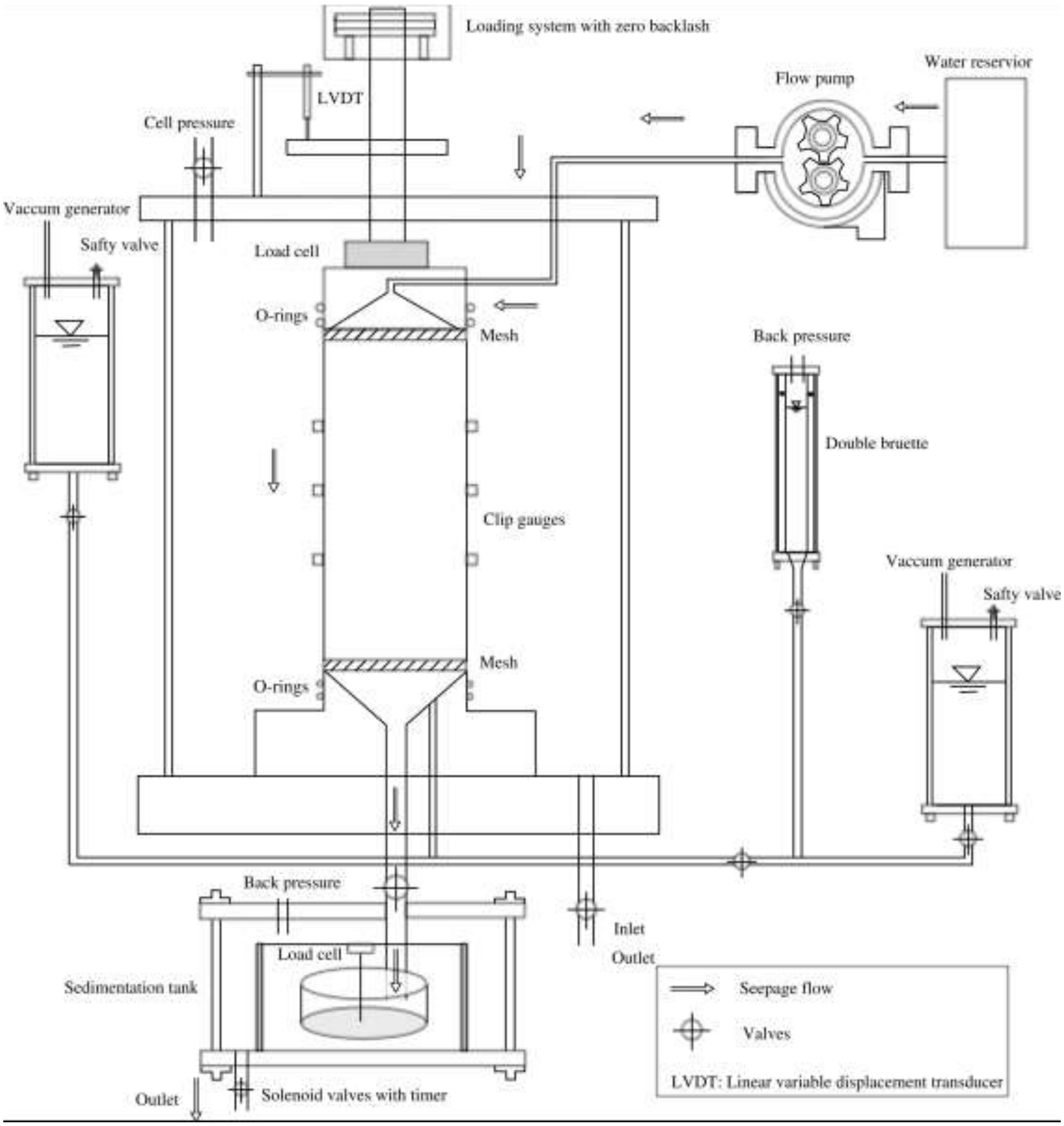

Fig. 3. Revised triaxial apparatus for seepage test

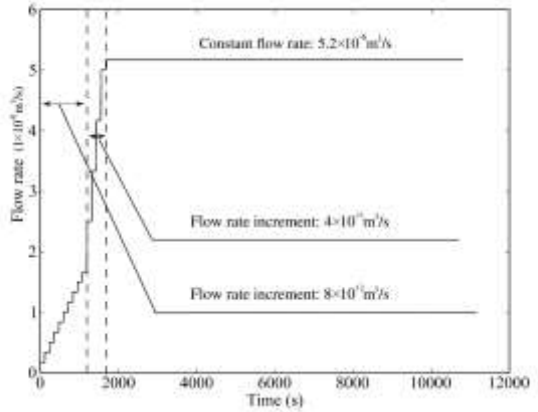

Fig. 4. Flow rate in seepage test

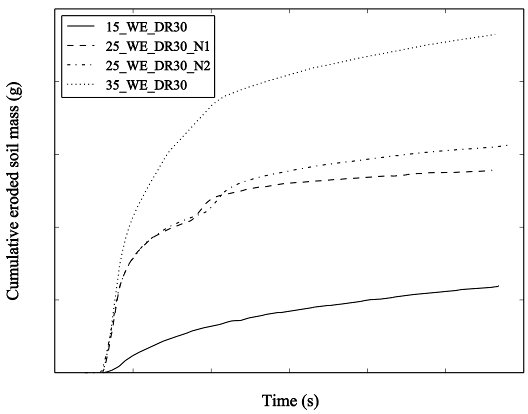

Fig. 5. Evolution of cumulative eroded soil mass during seepage test

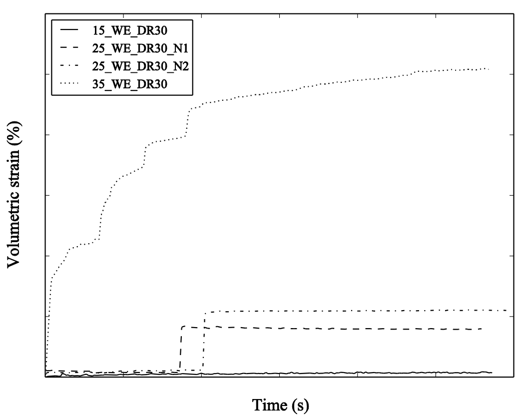

Fig. 6. Evolution of volumetric strain during seepage test

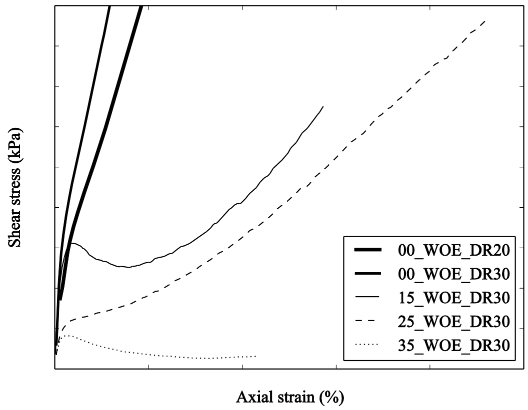

Fig. 7. Stress-strain curves of soils without erosion

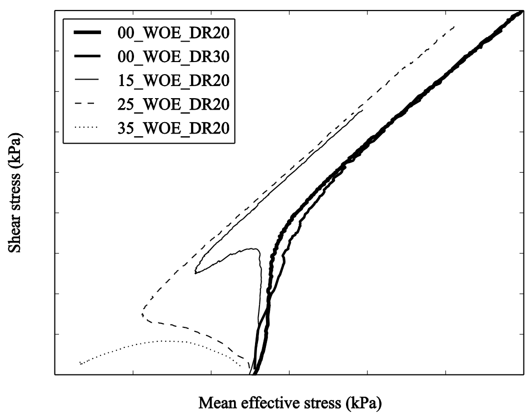

Fig. 8. Effective stress paths of soils without erosion

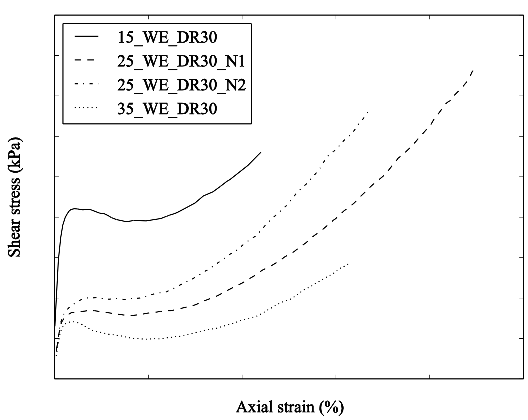

Fig. 9. Stress-strain curves of soils with erosion

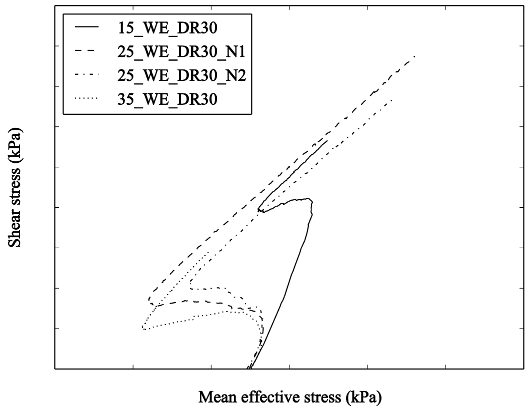

Fig. 10. Effective stress paths of soils with erosion

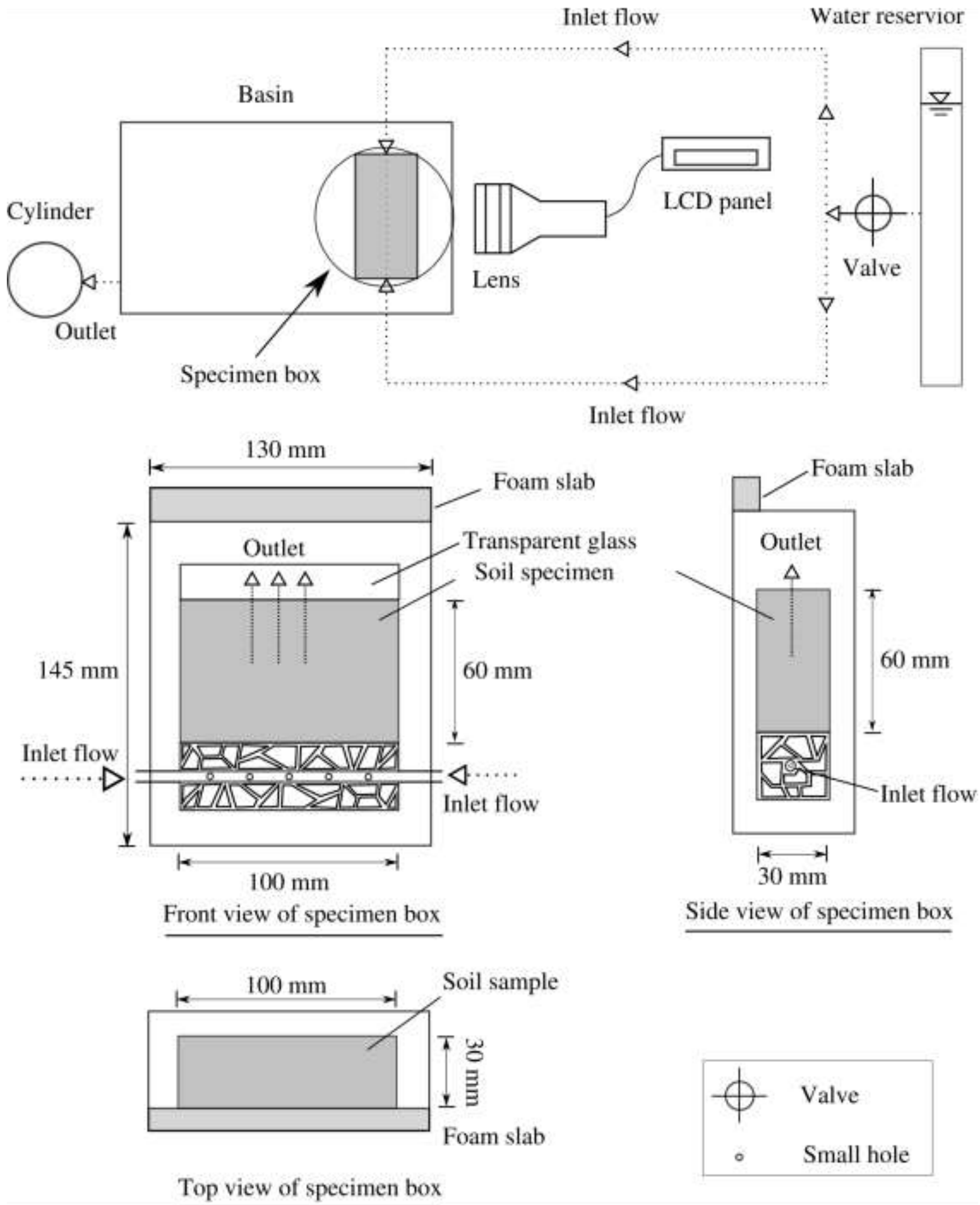

Fig. 11. Apparatus for upward seepage test

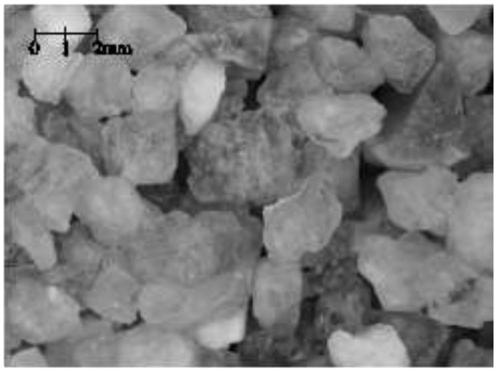

(a) Before erosion (0% initial fines content)

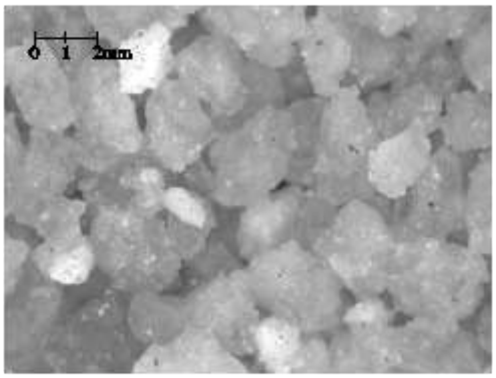

(b) Before erosion (15% initial fines content)

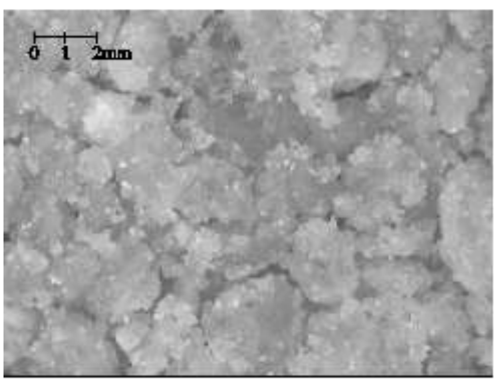

(c) Before erosion (25% initial fines content)

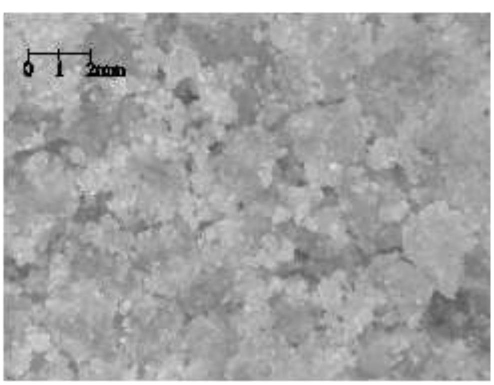

(d) Before erosion (35% initial fines content)

Fig. 12. Micro-structure of soils without erosion

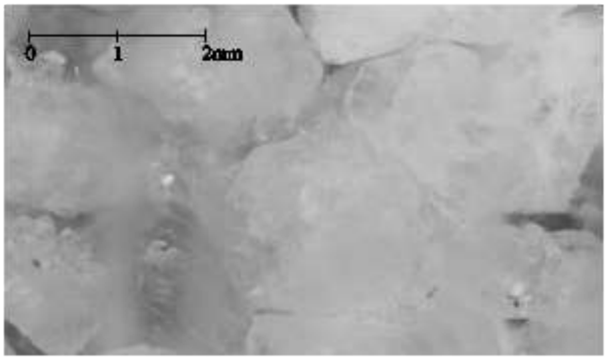

(a) After erosion (15% initial fines content)

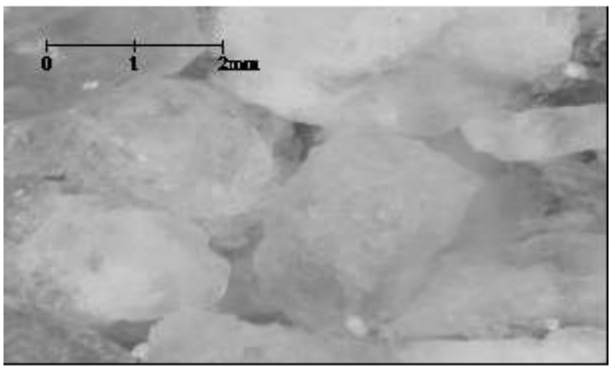

(b) After erosion (25% initial fines content)

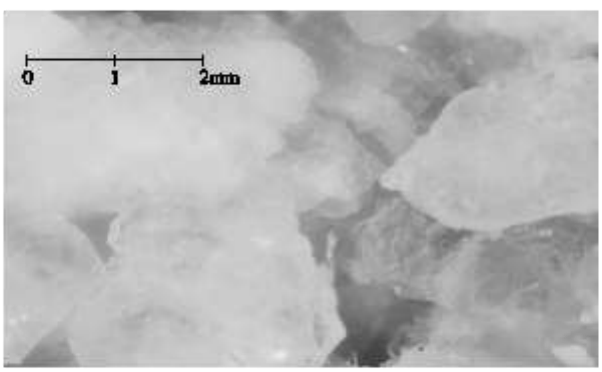

(c) After erosion (35% initial fines content)

Fig. 13. Micro-structure of soils with erosion

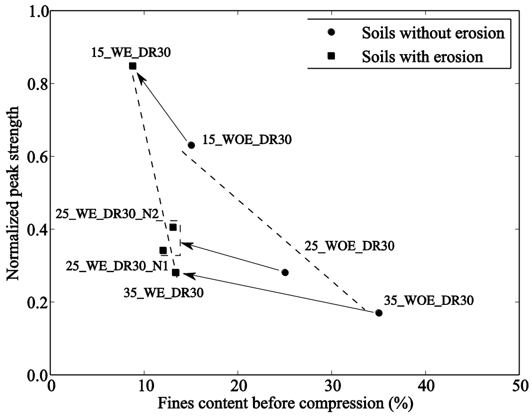

Fig. 14. Normalized peak strength against fines content before compression

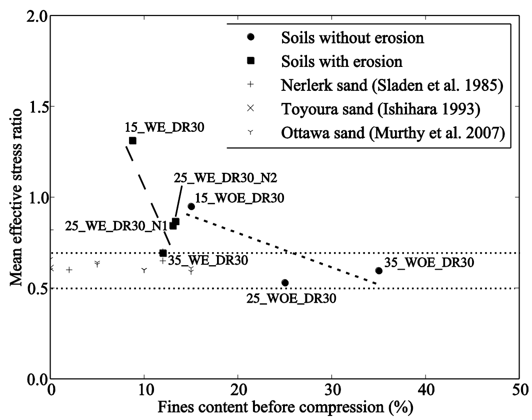

Fig. 15. Mean effective stress ratios against fines content before compression

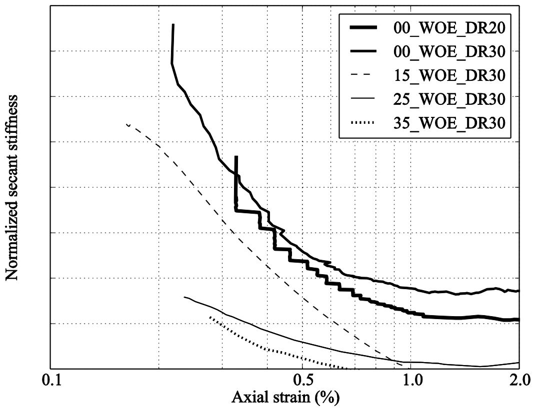

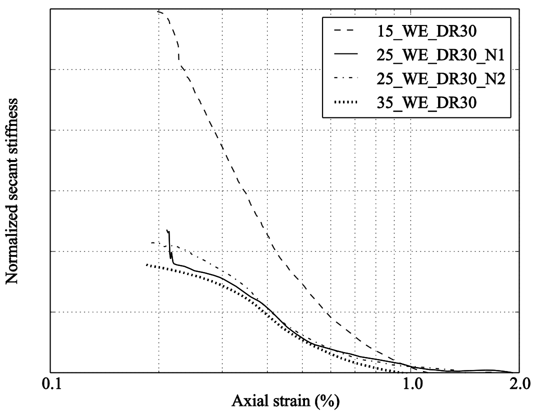

Fig. 16. Relation between normalized secant stiffness and axial strain

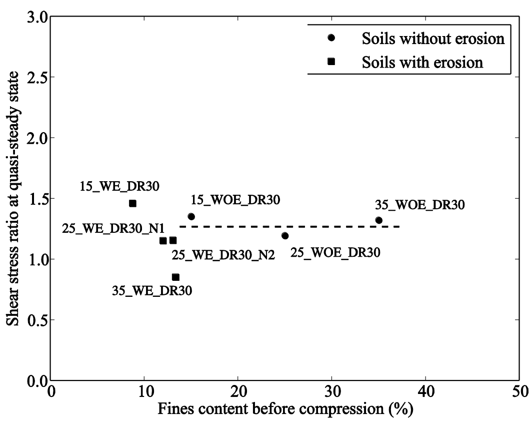

Fig. 17. Shear stress ratios at quasi-steady state against fines content before compression

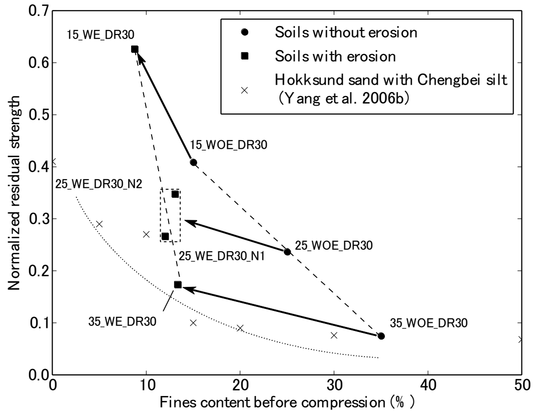

Fig. 18. Normalized residual strength against fines content before compression

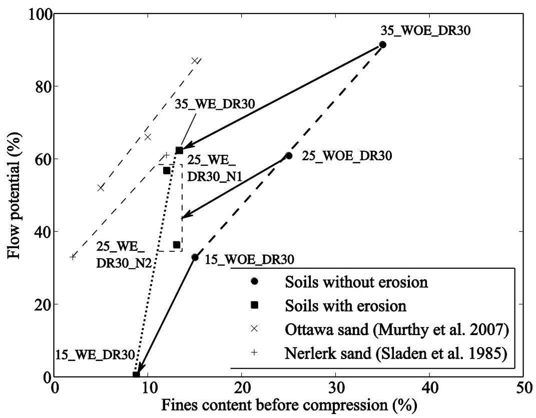

Fig. 19. Flow potential against fines content before compression

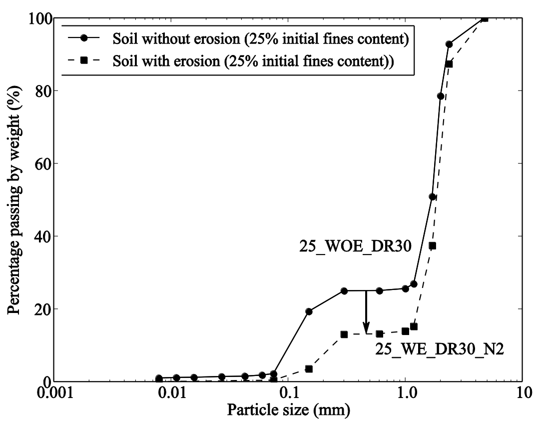

Fig. 20. Movement of particle grading curves

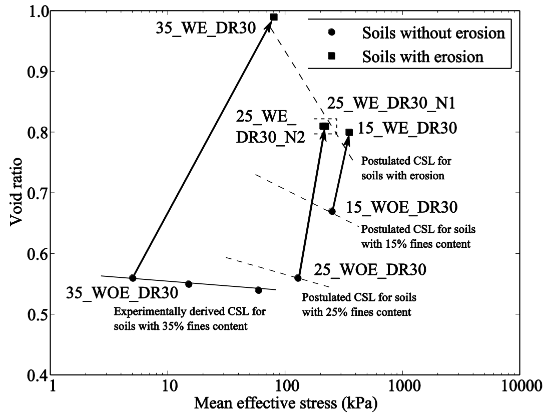

Fig. 21. Critical states of tested specimens in e-$logp'$ plane

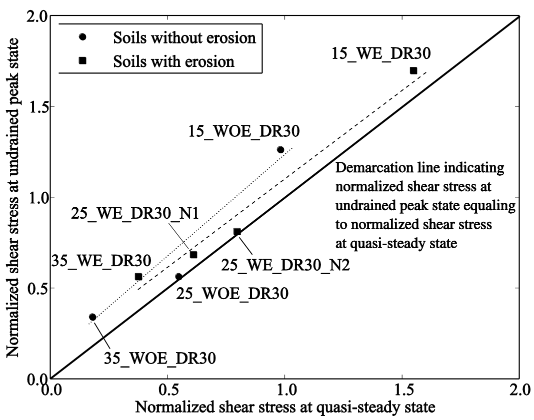

Fig. 22. Relation of normalized shear stress at undrained peak state and quasi-steady state

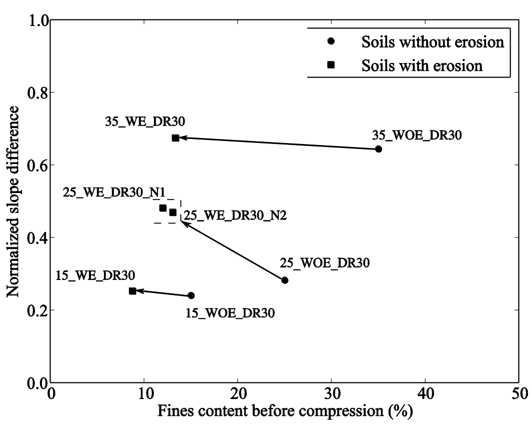

Fig. 23. Slope difference against fines content before compression

Appendix A. Extrapolation of critical state

The CSL is extrapolated by a four-parameter sigmoidal function proposed by Murthy et al. (2007). The function is expressed mathematically by

$$y = f(x) = a + \frac{b}{1 + e^{c(x-d)}} \tag{a1}$$

where, *a*, *b*, *c* and *d* are the fitting parameters.

Initially, the curve of the first deviation of mean effective stress $\partial p' / \partial \varepsilon_a$ against axial strain ε_a is plotted to find the stationary point, which is the projection of inflection in the relationship between axial strain ε_a and mean effective stress p'. Then, optimization was performed on both the ε_a - p' and $\partial p' / \partial \varepsilon_a$ - ε_a curves to get the fitting parameters of the sigmoidal function. To get the most reliable estimation of CSL, the global criterion method (Rao 2009) is utilized here. Figure A1 demonstrates the extrapolation process of the CSL of the uneroded soil containing 25% fines.

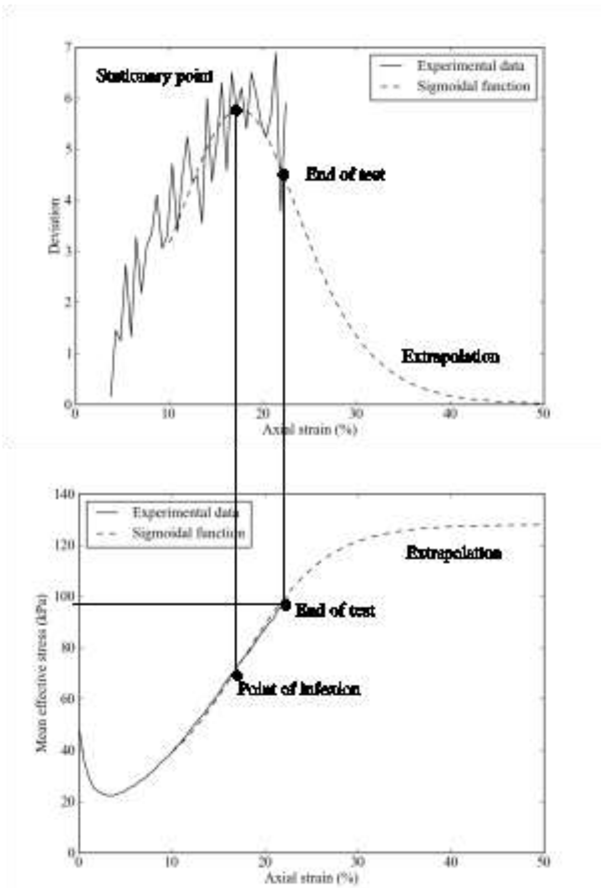

Fig. A1. Demonstration of the extrapolation of critical state